Nanotechnology Perceptions
ISSN 1660-6795
www.nano-*ntp.com*

Dual Phase-Lag Thermoelastic ModelingOf Rotating Orthotropic Viscothermoelastic Media With Two-Temperature And Hall Current Effects

Sandeep Kumar[1] and Rajneesh Kumar[2]

[1]Department of Mathematics, Chaudhary Devi Lal University, Sirsa, Haryana, India
[2]Department of Mathematics, Kurukshetra University, Kurukshetra, Haryana, India
Corresponding author: [1]goyat_sandeep30@yahoo.com, [2]rajneesh_kuk@rediffmail.com

This paper investigates the thermomechanical response of a rotating orthotropic viscothermoelastic medium incorporating dual-temperature and Hall current effects under mechanical and thermal loading conditions. The formulation is developed within the framework of Green–Naghdi type III thermoelasticity with dual phase-lag heat conduction, which accounts for finite thermal wave speeds and energy dissipation. The governing equations describing the coupled mechanical, thermal, and electromagnetic fields are solved using Laplace and Fourier transform techniques.To analyze the physical behavior, the bounding surface is subjected to both concentrated and linearly distributed mechanical and thermal sources. Analytical expressions for displacement components, stress distributions, conductive temperature, and current density are obtained in the transformed domain and subsequently inverted numerically to obtain solutions in the physical domain. Numerical simulations are presented to illustrate the influence of viscosity, rotation, and Hall current on the response characteristics.
The results reveal that all field quantities exhibit oscillatory behavior with distance from the boundary, with their nature strongly dependent on the type of applied source. The inclusion of viscosity significantly enhances the magnitude of responses near the boundary while increasing attenuation, thereby reducing the spatial extent of oscillations. The proposed model generalizes several existing theories as limiting cases and provides a comprehensive framework for analyzing coupled thermo-mechanical and electromagnetic effects in advanced materials.

Keywords: Green Nagdhi III; Viscothermoelastic; Orthotropic, Laplace and Fourier transform; Concentrated and distributed sources; Rotation; Hall current.

1. Introduction

In recent decades, considerable attention has been devoted to the development of generalized theories of thermoelasticity that account for the finite speed of thermal wave propagation. The classical theory of thermoelasticity, based on Fourier's law of heat conduction, predicts an infinite speed of heat propagation, which contradicts experimental observations, particularly in problems involving high heat fluxes and very short time intervals. To overcome this limitation, generalized thermoelastic theories were introduced. The pioneering works of Lord and Shulman [1] and Green and Lindsay [2] incorporated thermal relaxation times into the governing equations, thereby modifying the classical heat conduction law and eliminating the paradox of infinite thermal wave speed.

Subsequent developments led to hyperbolic formulations of thermoelasticity, which more accurately describe wave-type thermal propagation. A comprehensive review of such theories was presented by Chandrasekharaiah [46], emphasizing their importance in modern thermoelastic analysis. Green and Naghdi introduced a unified framework consisting of three distinct models (GN-I, GN-II, and GN-III) [3–5]. The GN-I model corresponds to classical thermoelasticity, while GN-II and GN-III allow for finite-speed thermal wave propagation without and with energy dissipation, respectively. These models have proven to be highly effective in analyzing dynamic thermoelastic phenomena.

An important extension of thermoelastic theory involves the concept of two temperatures. The two-temperature theory, originally proposed by Chen and Gurtin [6–8], distinguishes between conductive temperature and thermodynamic temperature, providing a more realistic description of heat transfer in non-equilibrium situations. Wave propagation under this framework was investigated by Warren and Chen [9], while significant advancements were later made by Youssef and co-workers [10–14]. Further contributions to wave propagation and thermoelastic response in two-temperature media were provided by several researchers, including Ezzat and Awad [15], Kaushal et al. [16, 19], and Sharma and collaborators [17–21], among others.

The influence of anisotropy and material inhomogeneity has also been extensively studied in thermoelastic media. Abbas et al. [22] investigated thermoelastic responses in transversely isotropic materials, demonstrating the significance of considering realistic material properties. Additional studies have highlighted the role of heat sources and relaxation effects in such materials [23, 24].

The combined effects of rotation and magnetic fields on thermoelastic wave propagation have attracted considerable attention due to their applications in geophysics, engineering, and material sciences. Several authors, including Kumar and Rupender [25], Kumar and Devi [26], Mahmoud [27], and Das and Kanoria [28], have analyzed magneto-thermoelastic interactions in rotating media. The presence of a magnetic field introduces coupling between thermal, mechanical, and electromagnetic fields, significantly influencing wave propagation behavior.

In realistic materials, viscoelastic effects must also be considered, as most solids exhibit time-dependent deformation under dynamic loading conditions. The importance of rheological behavior in thermal stress analysis was first emphasized by Freudenthal [29]. Later developments in thermoviscoelasticity were advanced through models such as Kelvin–Voigt and Maxwell-type formulations by Ieşan and Scalia [30], Borrelli and Patria [31], and further studies on wave propagation and material behavior [32–38]. Additional contributions by Hilton [39], Al-Basyouni et al. [40], and Yadav et al. [41] extended these models to include fractional-order effects and complex thermal loading conditions.

When the magnetic field is strong, the Hall current effect becomes important and alters the electrical conductivity of the medium. This effect induces currents perpendicular to both electric and magnetic fields. The influence of Hall current on thermoelastic interactions has been examined by various researchers such as Zakaria [42,44], Sarkar and Lahiri [43], and Kumar et al. [45], demonstrating its significant impact on magneto-thermoelastic coupling.

Recent research has focused on the combined effects of Hall current, rotation, and phase-lag heat conduction in generalized thermoelastic media. Kumar et al. [47] studied the influence of Hall current and two-temperature theory in transversely isotropic media. Lata [48]

investigated thermoelastic responses under concentrated forces, while Ezzat and El-Bary [49] and Ezzat et al. [50] developed fractional and phase-lag thermoelastic models within the Green–Naghdi framework. Furthermore, Lata and Kaur [51] examined the effects of Hall current and rotation in magneto-thermoelastic media.

Despite extensive research in generalized thermoelasticity, the combined effects of two-temperature theory, viscoelasticity, rotation, and Hall current in orthotropic media remain largely unexplored.

Motivated by this gap, the present study investigates the thermo-mechanical response of a rotating orthotropic viscothermoelastic medium within the framework of Green–Naghdi type-III theory, incorporating dual phase lags, two-temperature effects, and Hall current. The governing equations are formulated and solved using Laplace and Fourier transform techniques. Analytical expressions for displacement components, stress distributions, conductive temperature, and current density are obtained in the transformed domain. Numerical inversion methods, such as those proposed by Honig and Hirdes [54] and Press et al. [55], are employed to evaluate the physical behavior of the system under various loading conditions.

The results provide significant insights into the coupled effects of viscosity, rotation, magnetic field, and two-temperature parameters, with potential applications in geophysics, nuclear engineering, and advanced material systems.

2. Basic Equations

The constitutive relations for a transversely isotropic thermoelastic medium are given by

$$t_{ij} = C_{ijkl}e_{kl} - \beta_{ij}T \qquad (1)$$

Equation of motion for a transversely isotropic thermoelastic medium rotating uniformly with an angular velocity $\boldsymbol{\Omega} = \Omega n$, where n is a unit vector representing the direction of axis of rotation and taking into account Lorentz force

$$t_{ij,j} + F_i = \rho\{\ddot{u}_i + \left(\Omega \times (\Omega \times u)\right)_i + (2\Omega \times \dot{u})_i\} \qquad (2)$$

Following Chandrasekharaiah [46] and Youssef [10], The heat conduction equation with two temperature and with and without energy dissipation is given by

$$K_{ij}^{*}(1 + \tau_T \frac{\partial}{\partial t})\varphi_{,ij} + K_{ij}\dot{\varphi}_{ij} = \left(1 + \tau_q \frac{\partial}{\partial t} + \frac{\tau_q^2}{2!}\frac{\partial^2}{\partial t^2}\right)(\beta_{ij}T_0\ddot{e_{ij}} + \rho C_E\ddot{T}) \quad (3)$$

The above equations are supplemented by generalized Ohm's law for media with finite conductivity and including the Hall current effect

$$\mathbf{J} = \frac{\sigma_0}{1+m^2}\left(\mathbf{E} + \mu_0\left(\dot{\mathbf{u}} \times \mathbf{H} - \frac{1}{en_e}\mathbf{J} \times \mathbf{H}_0\right)\right) \qquad (4)$$

and the strain displacement relations are

$$e_{ij} = \frac{1}{2}(u_{i,j} + u_{j,i}) \qquad i,j = 1,2,3 \qquad (5)$$

Here

$F_i = \mu_0(\mathbf{J} \times \mathbf{H}_0)_i$, are the components of Lorentz force.

$\beta_{ij} = C_{ijkl}\alpha_{ij}$ and $T = \varphi - a_{ij}\varphi_{,ij}$

$\beta_{ij} = \beta_i\delta_{ij}$, $K_{ij} = K_i\delta_{ij}$, $K_{ij}^{*} = K_i^{*}\delta_{ij}$, i is not summed

$C_{ijkl}\left(C_{ijkl} = C_{klij} = C_{jikl} = C_{ijlk}\right)$ are elastic parameters, β_{ij} is the thermal tensor, T is the temperature, T_0 is the reference temperature, t_{ij} are the components of stress tensor, e_{kl} are

the components of strain tensor,u_i are the displacement components, ρ is the density, C_E is the specific heat, K_{ij} is the thermal conductivity, $K_{IJ}^*$is the materialistic constant, a_{ij} are the two temperature parameters, α_{ij} is the coefficient of linear thermal expansion, τ_T, τ_q denote relaxation times,Ω is the angular velocity of the solid, H is the magnetic strength, $\dot{\mathbf{u}}$ is the velocity vector , **E** is the intensity vector of the electric field, **J** is the current density vector, $m(=\omega_e t_e=\frac{\sigma_0\mu_0 H_0}{en_e})$ is the Hall parameter, t_e is the electron collision time, $\omega_e=\frac{e\mu_0 H_0}{m_e}$ is the electronic frequency, e is the charge of an electron, m_e is the mass of the electron, $\sigma_0=\frac{e^2 t_e n_e}{m_e}$, is the electrical conductivity and n_e is the number of density of electrons.

3. Formulation and Solution

We consider a homogeneous perfectly conducting orthotropic magneto- viscothermoelastic with dual phase lag model of Green Nagdhi III which is rotating uniformly with an angular velocity $\boldsymbol{\Omega}$ initially at uniform temperature T_0 . The rectangular Cartesian co-ordinate system (u_1, u_2, u_3) having origin on the surface (x_3=0) with x_3-axis pointing vertically into the medium is introduced. The surface of the half-space is subjected to thermomechanical sources. For two dimensional problem in $x_1 - x_3$ plane, we take

$$\mathbf{u} = (u_1, 0, u_3). \tag{6}$$

We also assume that

$$\mathbf{E}=0, \quad \boldsymbol{\Omega} = (0, \Omega, 0). \tag{7}$$

The generalized Ohm's law

$$J_2 = 0 \tag{8}$$

the current density components J_1 and J_3using (4) are given as

$$J_1 = \frac{\sigma_0\mu_0 H_0}{1+m^2}\left(m\frac{\partial u_1}{\partial t} - \frac{\partial u_3}{\partial t}\right) \tag{9}$$

$$J_3 = \frac{\sigma_0\mu_0 H_0}{1+m^2}\left(\frac{\partial u_1}{\partial t} + m\frac{\partial u_3}{\partial t}\right) \tag{10}$$

Following Slaughter [52], using appropriate transformations, on the set of equations (2) and (3) and with the aid of (6)-(10), we obtain the equations for orthotropic thermoelastic solid as

$$c_{11}\frac{\partial^2 u_1}{\partial x^2} + c_{13}\frac{\partial^2 u_3}{\partial x_1 \partial x_3} + c_{55}\left(\frac{\partial^2 u_1}{\partial {x_3}^2} + \frac{\partial^2 u_3}{\partial x_1 \partial x_3}\right) - \beta_1\frac{\partial}{\partial x_1}\left\{\varphi - \left(a_1\frac{\partial^2\varphi}{\partial {x_1}^2} + a_3\frac{\partial^2\varphi}{\partial {x_3}^2}\right)\right\} - \mu_0 J_3 H_0 = \rho\left(\frac{\partial^2 u_1}{\partial t^2} - \Omega^2 u_1 + 2\Omega\frac{\partial u_3}{\partial t}\right) \tag{11}$$

$$(c_{13}+c_{44})\frac{\partial^2 u_1}{\partial x_1 \partial x_3} + c_{55}\frac{\partial^2 u_3}{\partial {x_1}^2} + c_{33}\frac{\partial^2 u_3}{\partial {x_3}^2} - \beta_3\frac{\partial}{\partial x_3}\left\{\varphi - \left(a_1\frac{\partial^2\varphi}{\partial {x_1}^2} + a_3\frac{\partial^2\varphi}{\partial {x_3}^2}\right)\right\} + \mu_0 J_1 H_0 = \rho\left(\frac{\partial^2 u_3}{\partial t^2} - \Omega^2 u_3 - 2\Omega\frac{\partial u_1}{\partial t}\right) \tag{12}$$

$$\left({k_1}^*\left(1 + \tau_T\frac{\partial}{\partial t}\right) + k_1\frac{\partial}{\partial t}\right)\frac{\partial^2\varphi}{\partial {x_1}^2} + \left({k_3}^*\left(1 + \tau_T\frac{\partial}{\partial t}\right) + k_3\frac{\partial}{\partial t}\right)\frac{\partial^2\varphi}{\partial {x_3}^2} = \left(1 + \tau_q\frac{\partial}{\partial t} + \frac{\tau_q^2}{2!}\frac{\partial^2}{\partial t^2}\right)\left[T_0\frac{\partial^2}{\partial t^2}\left\{\beta_1\frac{\partial u_1}{\partial x_1} + \beta_3\frac{\partial u_3}{\partial x_3}\right\} + \rho C_E\ddot{T}\right] \tag{13}$$

and

$$t_{11} = c_{11}u_{1,1} + c_{13}u_{3,3} - \beta_1 T \tag{14}$$

$$t_{33} = c_{13}u_{1,1} + c_{33}u_{3,3} - \beta_3 T \tag{15}$$

$$t_{13} = 2c_{55}u_{1,3} \tag{16}$$

where

$$T = \varphi - \left(a_1 \frac{\partial^2 \varphi}{\partial x_1^2} + a_3 \frac{\partial^2 \varphi}{\partial x_3^2}\right)$$

$$\beta_1 = c_{11}\alpha_1 + c_{13}\alpha_3 , \qquad \beta_3 = c_{13}\alpha_1 + c_{33}\alpha_3$$

In the above equations we use the contracting subscript notations $(1 \to 11, 2 \to 22, 3 \to 33, 4 \to 23, 5 \to 31, 6 \to 12)$ to relate c_{ijkl} to c_{mn} .

To incorporate the damping characteristics of the medium, the material parameters are assumed to depend on the time differential operator $D = \frac{\partial}{\partial t}$ .Under the assumption of a Voigt-type linear viscoelastic model (Kaliski[53]), the constitutive coefficients take the form

$$c_{ij}(D) = c_{ij}^{*}(1 + Q_i D), \tag{17}$$

where $Q_i (i=1,2,3,4,5)$ are viscoelastic relaxation times.

For the present formulation, we have

$$c_{11} = {c_{11}}^{*}\left(1 + Q_1 \frac{\partial}{\partial t}\right), \quad c_{12} = {c_{12}}^{*}\left(1 + Q_2 \frac{\partial}{\partial t}\right), \; c_{13} = {c_{13}}^{*}\left(1 + Q_3 \frac{\partial}{\partial t}\right), \quad c_{33} = {c_{33}}^{*}\left(1 + Q_4 \frac{\partial}{\partial t}\right)$$

$$c_{55} = {c_{55}}^{*}\left(1 + Q_5 \frac{\partial}{\partial t}\right). \tag{18}$$

We assume that medium is initially at rest. The undisturbed state is maintained at reference temperature. Then we have the initial and regularity conditions are given by

$$u_1(x_1, x_3, 0) = 0 = \dot{u_1}(x_1, x_3, 0)$$
$$u_3(x_1, x_3, 0) = 0 = \dot{u_3}(x_1, x_3, 0)$$
$$\varphi(x_1, x_3, 0) = 0 = \dot{\varphi}(x_1, x_3, 0) \qquad \text{For } x_3 \geq 0, \quad -\infty < x_1 < \infty$$
$$u_1(x_1, x_3, t) = u_3(x_1, x_3, t) = \varphi(x_1, x_3, t) = 0 \text{ for } t > 0 \text{ when } x_3 \to \infty \tag{19}$$

To facilitate the solution, following dimensionless quantities are introduced:

$$x_1' = \frac{x_1}{L}, \; x_3' = \frac{x_3}{L}, \; u_1' = \frac{\rho c_1^2}{L\beta_1 T_0} u_1, \; u_3' = \frac{\rho c_1^2}{L\beta_1 T_0} u_3, \; T' = \frac{T}{T_0}, \; t' = \frac{c_1}{L} t, \; t_{11}' = \frac{t_{11}}{\beta_1 T_0}, \; J' = \frac{\rho c_1^2}{\beta_1 T_0} J,$$

$$t_{33}' = \frac{t_{33}}{\beta_1 T_0}, \; t_{31}' = \frac{t_{31}}{\beta_1 T_0}, \; \varphi' = \frac{\varphi}{T_0}, \; a_1' = \frac{a_1}{L^2}, \; a_3' = \frac{a_3}{L^2}, \quad h' = \frac{h}{H_0}, \; M = \frac{\sigma_0 \mu_0 H_0}{\rho c_1 L}, \; \Omega' = \frac{L}{c_1}\Omega \tag{20}$$

Making use of (18) in equations (11)- (13), after suppressing the primes, yield

$$\frac{\partial^2 u_1}{\partial {x_1}^2} + \delta_4 \frac{\partial^2 u_3}{\partial x_1 \partial x_3} + \delta_2 \left(\frac{\partial^2 u_1}{\partial {x_3}^2} + \frac{\partial^2 u_3}{\partial x_1 \partial x_3}\right) - \frac{\partial}{\partial x_1}\left\{\varphi - \left(a_1 \frac{\partial^2 \varphi}{\partial {x_1}^2} + a_3 \frac{\partial^2 \varphi}{\partial {x_3}^2}\right)\right\} - \frac{M}{1+m^2}\mu_0 H_0 \left(\frac{\partial u_1}{\partial t} + m \frac{\partial u_3}{\partial t}\right) = \frac{\partial^2 u_1}{\partial t^2} - \Omega^2 u_1 + 2\Omega \frac{\partial u_3}{\partial t} \tag{21}$$

$$\delta_1 \frac{\partial^2 u_1}{\partial x_1 \partial x_3} + \delta_2 \frac{\partial^2 u_3}{\partial {x_1}^2} + \delta_3 \frac{\partial^2 u_3}{\partial {x_3}^2} - \frac{\beta_3}{\beta_1}\frac{\partial}{\partial x_3}\left\{\varphi - \left(a_1 \frac{\partial^2 \varphi}{\partial {x_1}^2} + a_3 \frac{\partial^2 \varphi}{\partial {x_3}^2}\right)\right\} + \frac{M}{1+m^2}\mu_0 H_0 \left(m \frac{\partial u_1}{\partial t} - \frac{\partial u_3}{\partial t}\right) = \frac{\partial^2 u_3}{\partial t^2} - \Omega^2 u_3 - 2\Omega \frac{\partial u_1}{\partial t} \tag{22}$$

$$\varepsilon_1 \left(1 + \frac{\varepsilon_3}{\varepsilon_1}\frac{\partial}{\partial t}\right)\frac{\partial^2 \varphi}{\partial {x_1}^2} +$$

$$\varepsilon_2\left(1+\frac{\varepsilon_4}{\varepsilon_2}\frac{\partial}{\partial t}\right)\frac{\partial^2\varphi}{\partial {x_3}^2}=\left(1+\tau_q\ \frac{\partial}{\partial t}+\frac{\tau_q^2}{2!}\frac{\partial^2}{\partial t^2}\right)\ [\varepsilon_5{\beta_1}^2\frac{\partial^2}{\partial t^2}\left(\frac{\partial u_1}{\partial x_1}+\frac{\beta_3}{\beta_1}\frac{\partial u_3}{\partial x_3}\right)\ +\ \frac{\partial^2}{\partial t^2}\left(\left\{\varphi-a_1\frac{\partial^2\varphi}{\partial {x_1}^2}+a_3\frac{\partial^2\varphi}{\partial {x_3}^2}\right\}\right)] \quad (23)$$

$\delta_1=\frac{(c_{13}+c_{55})}{c_{11}}$, $\delta_2=\frac{c_{55}}{c_{11}}$, $\delta_3=\frac{c_{33}}{c_{11}}$, $\delta_4=\frac{c_{13}}{c_{11}}$, $\varepsilon_1=\frac{{k_1}^*(1+\tau_T\frac{\partial}{\partial t})}{\rho C_E c_1^2}$, $\varepsilon_2=\frac{{k_3}^*(1+\tau_T\frac{\partial}{\partial t})}{\rho C_E c_1^2}$, $\varepsilon_3=\frac{k_1}{L\rho C_E c_1}$,

$\varepsilon_4=\frac{k_3}{L\rho C_E c_1}$, $\varepsilon_5=\frac{T_0}{\rho^2 C_E c_1^2}$.

Apply Laplace and Fourier transforms defined by

$$\bar{f}(x_1,x_3,s)=\int_0^\infty f(x_1,x_3,t)e^{-st}dt \quad (24)$$

$$\hat{f}(\xi,x_3,s)=\int_{-\infty}^{\infty}\bar{f}(x_1,x_3,s)e^{i\xi x_1}dx_1 \quad (25)$$

on equations (21)-(23), we obtain a system of homogeneous equations in terms of $\widetilde{u_1}, \widetilde{u_3}$ and $\tilde{\varphi}$ which yield a non trivial solution if determinant of coefficient $\{\widetilde{u_1}, \widetilde{u_3}, \tilde{\varphi}\}^T$ vanishes and we obtain the following characteristic equation

$$PD^6+QD^4+RD^2+S)(\widetilde{u_1},\widetilde{u_3},\tilde{\varphi})=0 \quad (26)$$

where,

P, Q, R and S are given in appendix A

The solution of the equation (26) satisfying the radiation condition that $\widetilde{u_1}, \widetilde{u_3}, \tilde{\varphi}\to 0$ as $x_3\to\infty$, can be written as

$$\hat{u}_1=A_1e^{-\lambda_1 x_3}+A_2e^{-\lambda_2 x_3}+A_3e^{-\lambda_3 x_3} \quad (27)$$

$$\hat{u}_3=d_1A_1e^{-\lambda_1 x_3}+d_2A_2e^{-\lambda_2 x_3}+d_3A_3e^{-\lambda_3 x_3} \quad (28)$$

$$\hat{\varphi}=l_1A_1e^{-\lambda_1 x_3}+l_2A_2e^{-\lambda_2 x_3}+l_3A_3e^{-\lambda_3 x_3} \quad (29)$$

where $\pm\lambda_i$, (i =1,2,3), are the roots of (26) and d_i and l_i are given in appendix B

4. Boundary Conditions

On the half-space surface ($x_3=0$), a normal mechanical load and a thermal source are applied. The corresponding boundary conditions are

(i) $t_{33}=-F_1\psi_1(x_1,t)$ (30)

(ii) $t_{31}=0$ (31)

(iii) $\frac{\partial\varphi}{\partial x_3}=F_2\psi_2(x_1,t)$ at $x_3=0$ (32)

where F_1 is the magnitude of the force applied, F_2 is the constant temperature applied on the boundary,

Two cases of source distribution are considered:

i) a continuously applied concentrated load/source,

ii) a continuously applied linearly distributed load/source.

5.1 Concentrated Source

For a continuous applied concentrated normal force and thermal source

$$\psi_i(x_1,,t) = \delta(x_1)H(t), \qquad i = 1,2 \qquad (33)$$

In equations (30) and (32). Applying the Laplace and Fourier transform defined by (24)-(25) on the equation (33) gives

$$\widehat{\psi}_i(\xi, s) = 1/s \quad , \quad i = 1,2 \qquad (34)$$

Using (34) in (C.1) -(C.7), we obtain the components of displacement, stress and conductive temperature and current density components.

5.2 Linearly Distributed Source

For a continuopusly applied linearly distributed normal force/ thermal source over the interval $|x_1| \le m_0$:

$$\psi_i(x_1, t) = H(t)\begin{cases} 1 - \frac{|x_1|}{m_0} \text{ if } |x_1| \le m_0 \\ 0 \text{ if } |x_1| > m_0 \end{cases}, i = 1,2 \qquad (35)$$

The corresponding Fourier- Laplace transforms are:

$$\widehat{\psi}_i(\xi, s) = \frac{1}{s}\left[2\,(1 - \cos(\xi m))\Big/_{(m_0\xi^2)}\right], \xi \neq 0, i = 1,2 \qquad (36)$$

Substituting the values of $\hat{u}_1$, $\hat{u}_3$ and $\hat{\varphi}$ in boundary conditions (30) –(32),and using (14)-(16),(20),(24) and(25), we obtain the expressions for displacement, stresses and conductive temperature and current density components as given in Appendix C [Eqs.(C.1)-(C.7)]

Using (34) in (C.1) -(C.7) , we obtain the corresponding expressions of field quantities or continuous applied concentrated normal force and thermal source.

The expressions for displacement, stresses and conductive temperature and current density components can be obtained for continuous applied linearly distributed normal force and thermal source by replacing $\widehat{\psi}_1(\xi, s)$ and $\widehat{\psi}_2(\xi, s)$ from (36) respectively in equations (C.1) -(C.7)

5(a) Mechanical Force.

Taking $F_2 = 0$ in equations (C.1) -(C.7), we obtain the components of displacement, normal stress, tangential stress, conductive temperature and current density components due to mechanical force.

5(b) Thermal Source.

Taking $F_1 = 0$ in equations (C.1) -(C.7), we obtain the components of displacement, normal stress, tangential stress, conductive temperature and current density components due to thermal source.

6. Particular cases

(i) If $a_1 = a_3 = 0$, then from (C.1) -(C.7), we obtain the corresponding expressions for displacements, stresses, conductive temperature and components of current density for orthotropic magneto- viscothermoelastic solid with dual phase lag GN-III formulation along with Hall current effect and rotation.

(ii) If we take $c_{11} = \lambda + 2\mu = c_{33}$, $c_{12} = c_{13} = \lambda$, $c_{55} = \mu$, $\beta_1 = \beta_3 = \beta$, $\alpha_1 = \alpha_3 = \alpha$, $K_1 = K_3 = K$ in equations(C.1)-(C.7), we obtain the corresponding expressions for displacements, stresses , conductive temperature components of current density in isotropic

magneto-thermoelastic solid with two temperature with dual phase lag GN-III model along with combined effects of Hall current and rotation.

(iii) If m=0, in equations (C.1) -(C.7), we obtain the components of displacements, stresses, conductive temperature and components of current density for orthotropic magneto-thermoelastic with dual phase lag GN-III model and with two temperature along with rotation.

(iv) If k_1=$k_3 = 0$ in equations (C.1) -(C.7), the corresponding results are recovered for orthotropic magneto- viscothermoelastic with rotation in case of dual phase lags GN II model.

(v) If τ_T=τ_q=0 in equations (C.1) -(C.7), determine the results for orthotropic magneto-viscothermoelastic with rotation in case of with and without energy dissipation for GN-III and GN-II model respectively.

Our results are in agreement for all the particular cases, if we solve the problem directly.

7. Inversion of the Transformation

To obtain the solution of the problem in physical domain, we must invert the transforms in equations (C.1)-(C.7). Here the displacement components, normal and tangential stresses and conductive temperature are functions of x_3, the parameters of Laplace and Fourier transforms s and ξ respectively and hence are of the form f (ξ, x_3, s). To obtain the function $f(x_1, x_3, t)$ in the physical domain, we first invert the Fourier transform using

$$\bar{f}(x_1, x_3, s)=\frac{1}{2\pi}\int_{-\infty}^{\infty} e^{-i\xi x_1}\,\hat{f}(\xi, x_3, s)d\xi = \frac{1}{2\pi}\int_{-\infty}^{\infty}|\cos(\xi x)\, f_e - i\sin(\xi x) f_o|\, d\xi \qquad (37)$$

Where f_e and $f_o$are respectively the odd and even parts of $\hat{f}(\xi, x_3, s)$. Thus the expression (37) gives the Laplace transform $\bar{f}(x_1, x_3, s)$ of the function $f(x_1, x_3, , t)$. Following Honig and Hirdes [54], the Laplace transform function $\bar{f}(x_1, x_3, s)$ can be inverted to $f(x_1, x_3, t)$.

The last step is to calculate the integral in equation (37). The method for evaluating this integral is described in Press et al. [55] . It involves the use of Romberg's integration with adaptive step size. This also uses the results from successive refinements of the extended trapezoidal rule followed by extrapolation of the results to the limit when the step size tends to zero.

8. Numerical results and discussion

For the purpose of numerical evaluation, cobalt material has been chosen following Dhaliwal and Singh [56], as

$c_{11} = 3.071 \times 10^{11}\mathrm{Nm}^{-2}$, $c_{33} = 3.581 \times 10^{11}\mathrm{Nm}^{-2}$, $c_{13} = 1.027 \times 10^{11}\mathrm{Nm}^{-2}$, $c_{55} = 1.510 \times 10^{11}\mathrm{Nm}^{-2}$, $\rho = 8.836 \times 10^{3}\mathrm{Kgm}^{-3}$, $T_0 = 298°\mathrm{K}$, $C_E = 4.27 \times 10^{2}\mathrm{JKg}^{-1}\mathrm{deg}^{-1}$, $K_1 = .690 \times 10^{2}\mathrm{wm}^{-1}\mathrm{deg}^{-1}$, $K_3 = .690 \times 10^{2}\mathrm{wm}^{-1}\mathrm{deg}^{-1}$, $\beta_1 = 7.04 \times 10^{6}\mathrm{Nm}^{-2}\mathrm{deg}^{-1}$, $\beta_3 = 6.90 \times 10^{6}\mathrm{Nm}^{-2}\mathrm{deg}^{-1}$, $K_1^* = 0.02 \times 10^{2}\mathrm{Nsec}^{-2}\mathrm{deg}^{-1}$, $K_3^* = 0.04 \times 10^{2}\mathrm{Nsec}^{-2}\mathrm{deg}^{-1}$, $\mu_0 = 1.2571 \times 10^{-6}\mathrm{Hm}^{-1}$, $H_0 = 1\mathrm{Jm}^{-1}\mathrm{nb}^{-1}$, $\varepsilon_0 = 8.838 \times 10^{-12}\mathrm{Fm}^{-1}$ with non-dimensional parameter L=1 and $\sigma_0 = 9.36 \times \frac{10^5\mathrm{col}^2}{\mathrm{Cal}}$. cm.sec, Ω=3, $t_0 = 0.02$, M=3, $m_0 = 1$, τ_T=0.02 , τ_q=0.04

and two temperature parameters are taken as a_1=0.03 and a_3=0.06

Using the above values, the graphical representations of stress components, conductive temperature and current density components for orthotropic magneto-viscothermoelastic

have been investigated due to thermomechanical sources. Effect of viscosity on the various quantities with distance x has been shown.

For viscoelastic medium we take the values $Q_1 = 0.5, Q_2 = 0.75, Q_3 = 1.0, Q_4 = 1.5, Q_5 = 2.0$ and for without viscoelastic, we take $Q_1 = Q_2 = Q_3 = Q_4 = Q_5 = 0$.

(i) Solid line represents the transversely isotropic magneto-thermoelastic with viscosity (VS)

(ii) Solid line with centre symbol circle represents transversely isotropic magneto-thermoelastic without viscosity (WVS)

In the graphical results, the spatial coordinate x represents x_1.

8.1 Concentrated normal force

Fig1. depicts variations of t_{33} with distance x. t_{33} exhibits an oscillatory variation with decreasing amplitude as the distance increases, indicating attenuation of the mechanical response away from the source. The presence of viscosity significantly increases the peak stress near the boundary while enhancing damping, resulting in faster decay of the response.

Fig. 2 presents the variations of t_{31} with x. t_{31} displays oscillatory behavior with diminishing amplitude, reflecting attenuation of shear effects with distance. Viscosity increases the peak values near the source and reduces the persistence of oscillations, highlighting its dissipative influence on the medium.

Fig.3 exhibits variations of φ with x. The magnitude of φ increases sharply in the near-field region ($0 \leq x \leq 2$) due to strong thermo-mechanical coupling at the boundary, followed by oscillatory decay at larger distances. The inclusion of viscosity increases the temperature magnitude and smoothens the decay profile, indicating enhanced thermal diffusion.

Fig 4. shows the variation of current density component J_1 with x . The current density exhibits oscillatory variation with decreasing amplitude, indicating attenuation of the electromagnetic response. Viscosity increases the initial magnitude near the boundary and accelerates the decay, demonstrating its damping effect on coupled field interactions.

Fig 5. shows the variation of current density component J_3 with x. The behavior is similar to that of J_1 , confirming consistency in the electromagnetic response of the medium. However, differences in magnitude reflect the anisotropic nature of the material. The presence of viscosity enhances peak values while reducing the spatial extent of oscillations.

8.2 Linearly distributed normal force

Fig.6 shows variation of t_{33} with x. It is noticed that t_{33} exhibits an oscillatory behavior with gradually increasing amplitude in the near-field region due to the distributed loading. Compared to the concentrated case, the response is smoother and more spatially extended. The presence of viscosity increases the stress magnitude while moderating the rate of oscillatory variation, indicating enhanced damping and redistribution of mechanical energy.

Fig.7 presents the variations of t_{31} with x. t_{31} displays oscillatory behavior with increasing amplitude in the near region, reflecting the cumulative shear effect induced by distributed loading. Viscosity enhances the magnitude of stress while reducing the spatial extent of oscillations, demonstrating its dissipative influence.

Fig8. exhibits variation of φ with x. φ exhibits oscillatory behavior with decreasing amplitude over the entire domain, indicating attenuation of the thermal response. Compared to the concentrated case, the variation is smoother due to the distributed nature of the source.

Viscosity increases the temperature magnitude while reducing fluctuations, reflecting enhanced thermal diffusion.

Fig 9 shows the variation of J_1 with x.The current densityJ_1 exhibits oscillatory variation with moderate amplitude, indicating coupled electromagnetic response. The inclusion of viscosity increases peak values near the boundary while reducing the spread of oscillations, demonstrating its damping effect.

Fig.10 shows the variation of J_3 with x.The behavior of J_3 is similar to that of J_1, confirming consistency in the electromagnetic response. Differences in magnitude arise due to anisotropic properties of the medium. Viscosity leads to higher peak values and enhanced attenuation of oscillations.

8.3 Concentrated thermal source

Fig. 11 shows the variation of t_{33} with x. t_{33} exhibits a pronounced increase in the vicinity of the source, followed by an oscillatory decay with distance. This behavior reflects the strong coupling between thermal loading and mechanical response near the boundary The inclusion of viscosity increases the peak stress magnitude while promoting faster attenuation, indicating enhanced dissipation of thermally induced stresses.

Fig.12 presents the variation of t_{31} with x. t_{31} initially decreases sharply in the near-field region $(0 \leq x \leq 2)$ and subsequently exhibits oscillatory behavior. This trend indicates rapid redistribution of thermally induced shear stresses. Viscosity amplifies the initial response and reduces the persistence of oscillations, highlighting its damping effect on shear deformation.

Fig13. exhibits variation of φ with x. φ increases rapidly near the source due to localized thermal input and then transitions into an oscillatory decay which indicates strong thermal gradients near the boundary. The presence of viscosity enhances the temperature magnitude and smoothens the spatial variation, reflecting increased thermal diffusion and energy dissipation.

Fig. 14 describe the variations of J_1 with x. The response is characterized by a sharp increase near the source followed by oscillatory attenuation. Viscosity increases the peak current density and accelerates its decay, demonstrating its role in damping the coupled field response.

Fig. 15 shows the variation of J_3 with x. The variation of J_3 follows a similar oscillatory pattern as J_1 , with differences primarily in magnitude due to anisotropic effects. The presence of viscosity enhances the peak response while reducing the spatial extent of oscillations, further confirming its damping influence on the electromagnetic behavior.

8.4 Linearly distributed thermal source

Fig.16 shows variations of t_{33} with x The response exhibits an oscillatory pattern with increasing magnitude in the near-field region, which can be attributed to the cumulative effect of thermal loading distributed over a finite interval. The presence of viscosity significantly increases the stress magnitude near the boundary while reducing the intensity of oscillations, indicating enhanced energy dissipation and redistribution.

Fig.17 presents the variations of t_{31} with x. t_{31} exhibits oscillatory behavior with a gradual increase in magnitude in the near region. Viscosity enhances the magnitude of the stress

without significantly altering the overall trend, suggesting that viscous effects primarily influence damping rather than the fundamental deformation pattern.

Fig.18 exhibits variation of φ vs x. φ exhibits smooth oscillatory behavior across the domain, indicating a more uniform thermal response compared to the concentrated source case. The distributed nature of the source reduces localized peaks and spreads the thermal effect. The inclusion of viscosity increases the temperature magnitude and suppresses fluctuations, reflecting enhanced thermal diffusion.

Fig19 describe the variations of J_1 vs x. J_1 decreases with distance in an oscillatory manner, indicating attenuation of the electromagnetic response. Viscosity increases the initial magnitude while accelerating attenuation, demonstrating its role in dissipating coupled field effects.

Fig20. describe the variation of J_3 vs x. The behavior is similar to that of J_1, confirming consistency in the electromagnetic response of the medium. However, differences in magnitude highlight the anisotropic characteristics of the material. The presence of viscosity leads to higher peak values and reduced oscillation range, emphasizing its damping influence.

Conclusion

This study presents a comprehensive analysis of the thermomechanical response of a rotating orthotropic viscothermoelastic medium incorporating dual-temperature and Hall current effects within the framework of Green–Naghdi type III theory with dual phase lag. The problem is solved using Laplace and Fourier transform techniques, enabling the evaluation of displacement, stress, temperature, and current density fields under mechanical and thermal loading conditions.

The results demonstrate that all field quantities exhibit oscillatory behavior with distance from the boundary, with characteristics strongly dependent on the nature of the applied sources. Concentrated sources produce sharp variations near the boundary, whereas linearly distributed sources yield smoother and more spatially extended responses.

A key finding is the significant role of viscosity, which increases the magnitude of field quantities near the boundary while enhancing attenuation, thereby reducing the spatial extent of oscillations. This confirms the damping nature of viscous effects in thermoelastic media. Furthermore, rotation and Hall current introduce strong coupling between mechanical, thermal, and electromagnetic fields, significantly influencing current density distribution, particularly under high magnetic field conditions.

The proposed formulation is general and reduces to several known models as limiting cases. The results provide useful insights for the analysis of materials and systems subjected to coupled thermomechanical and electromagnetic effects, with potential applications in geophysical media, rotating structures, and magneto-thermoelastic environments.

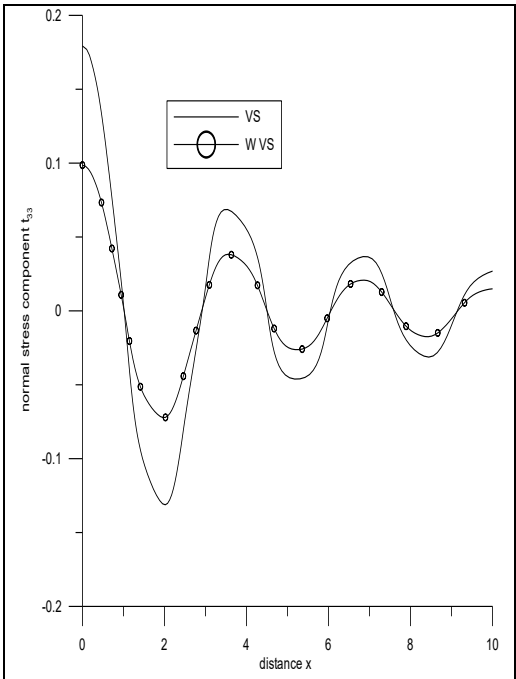

Fig.1Variation of t_{33} with x (concentrated normal force)

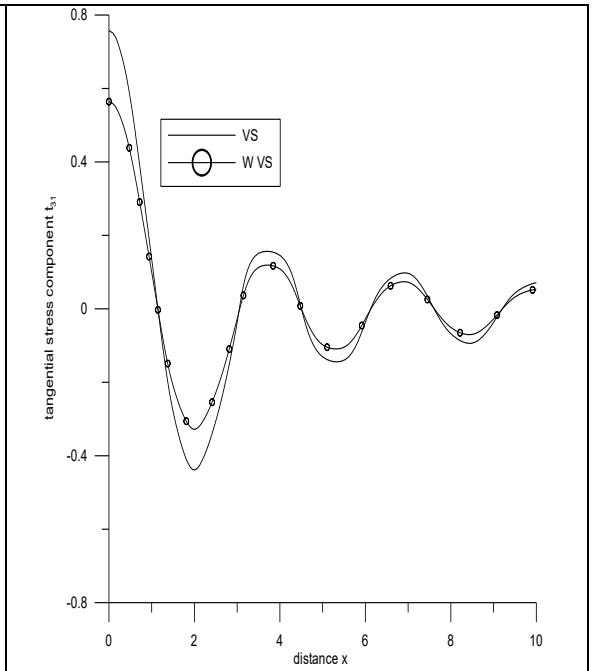

Fig.2.Variations of t_{31} with x (concentrated normal force)

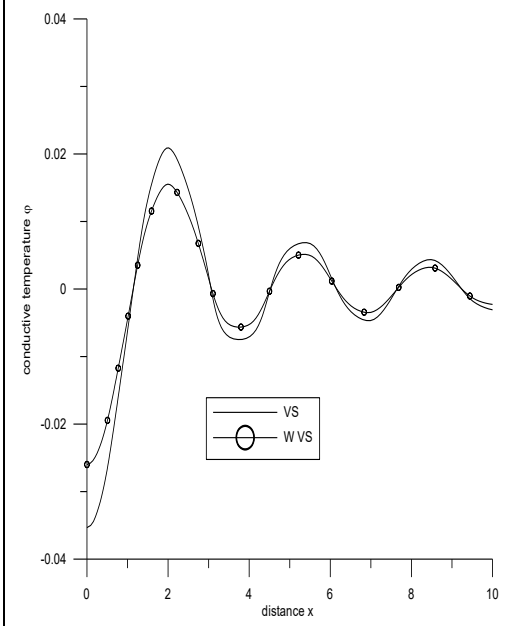

Fig.3.Variation of φ with x (concentrated normal force)

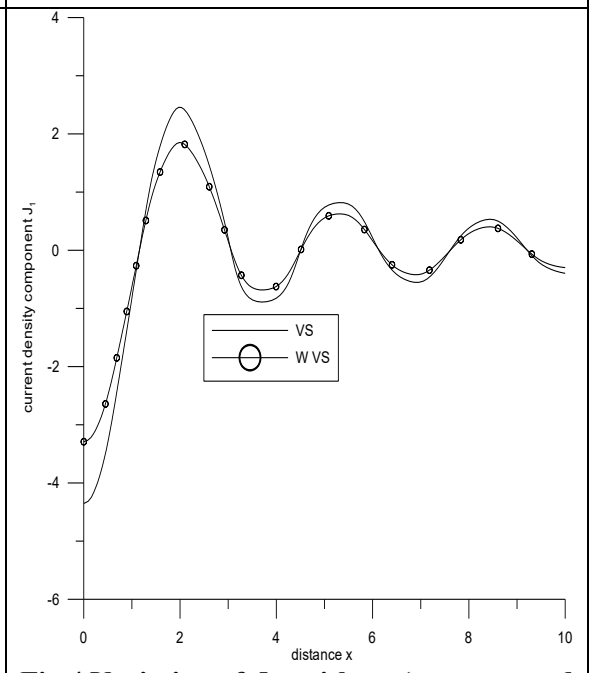

Fig.4.Variation of J_1 with x (concentrated normal force)

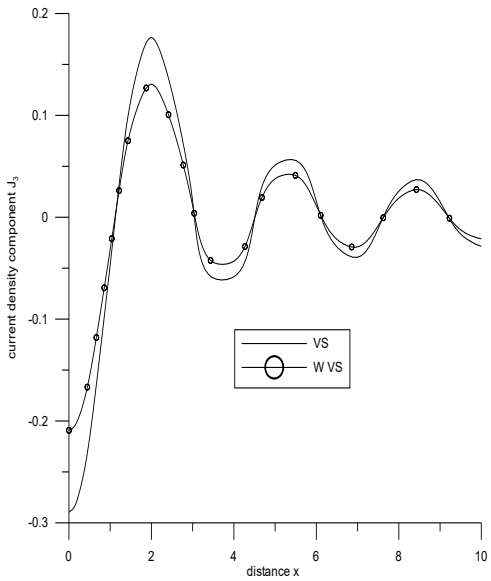

Fig.5. Variation of . J_3 with x (concentrated normal force)

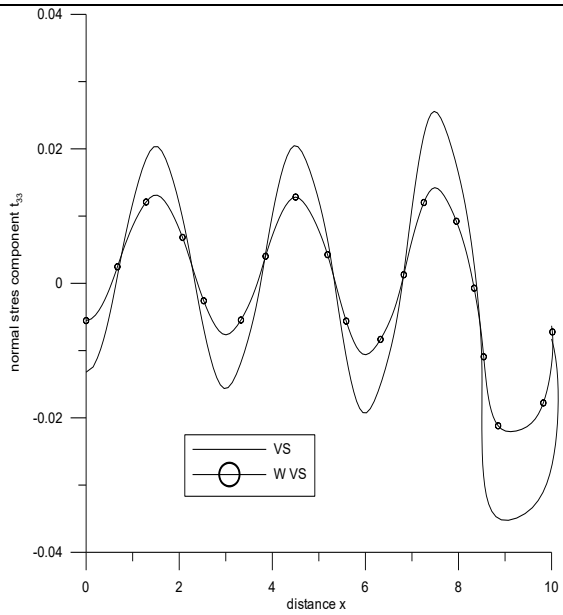

Fig.6. Variation of t_{33} with x (linearly distributed normal force)

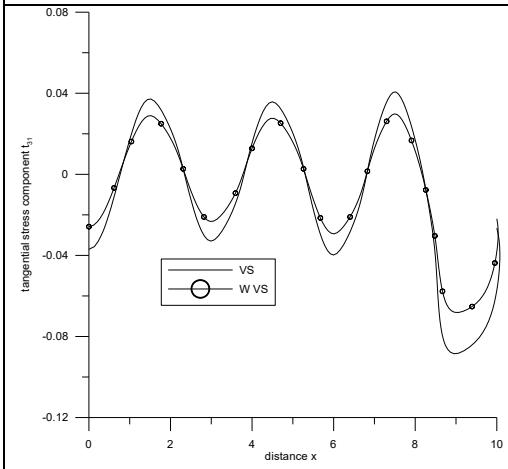

Fig.7. Variation of $t_{31}$with x (linearly distributed normal force)

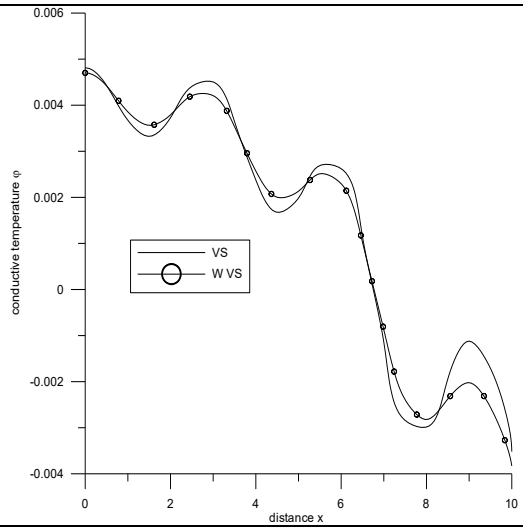

Fig.8. Variation of φ with x (linearly distributed normal force)

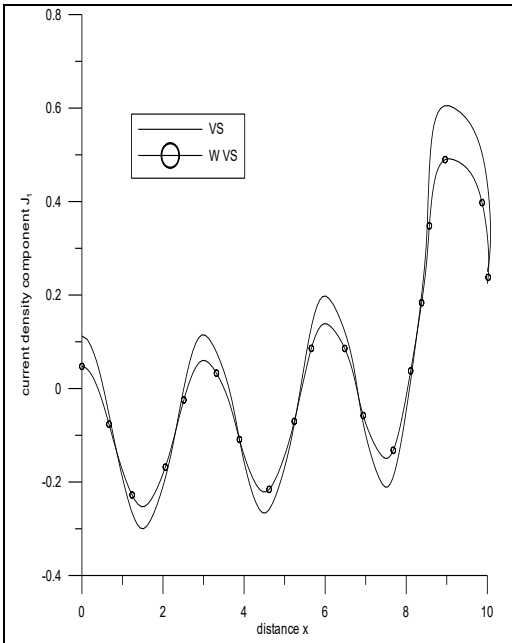

Fig.9. Variation of J_1 with x (linearly distributed normal force).

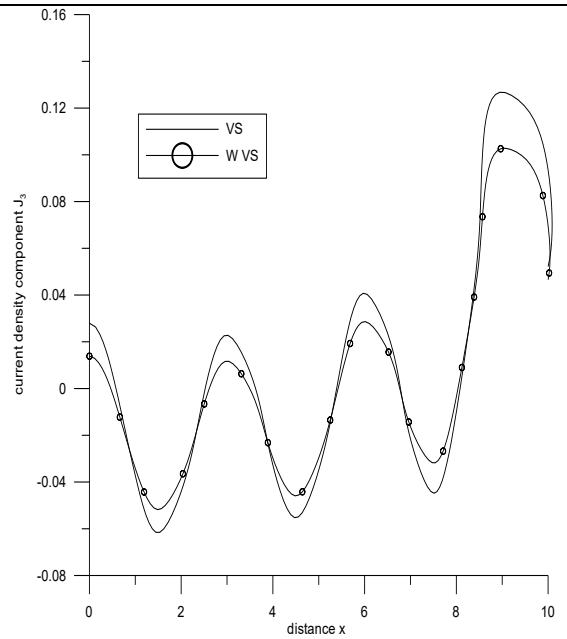

Fig.10. Variation of. J_3 with x (linearly distributed normal force).

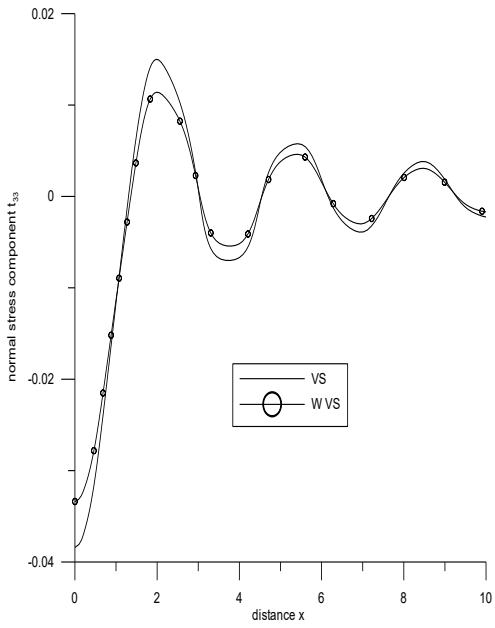

Fig.11.Variation of $t_{33}$with x (concentrated thermal source)

.

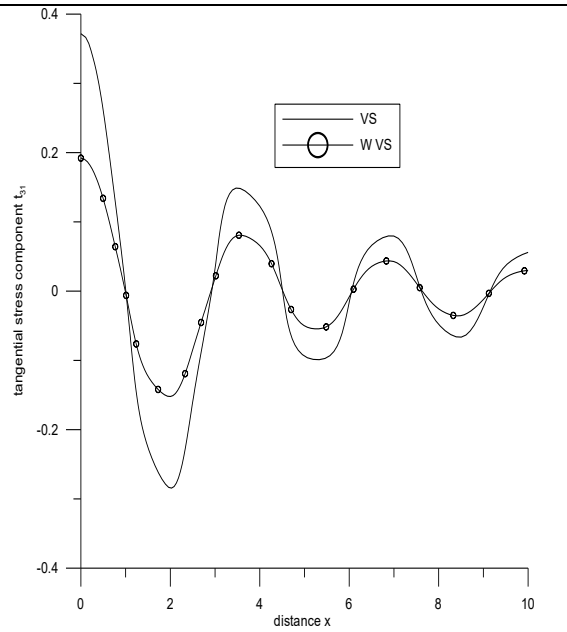

Fig.12. Variation of t_{31} with x (concentrated thermal source)

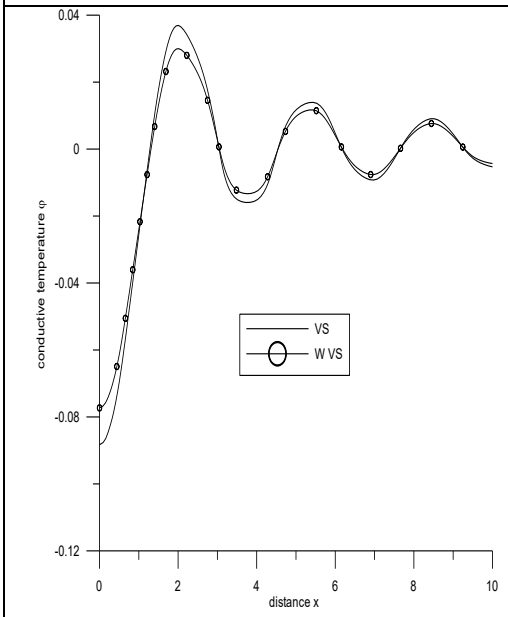

Fig.13. Variation of φ with x (concentrated thermal source)

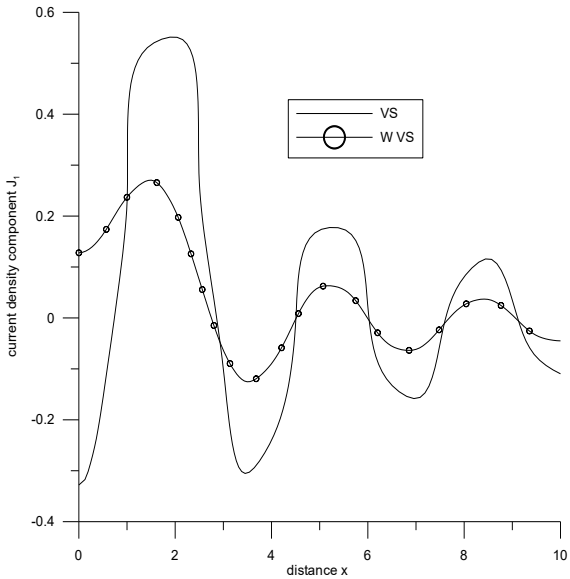

Fig. 14. Variation of J_1 with x (concentrated thermal source)

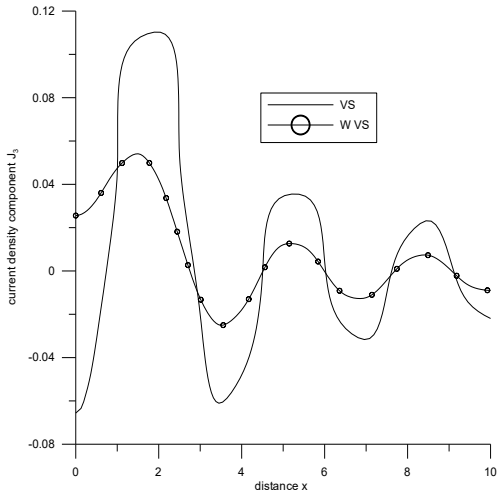

Fig.15 Variation of J_1 with x (concentrated thermal source)

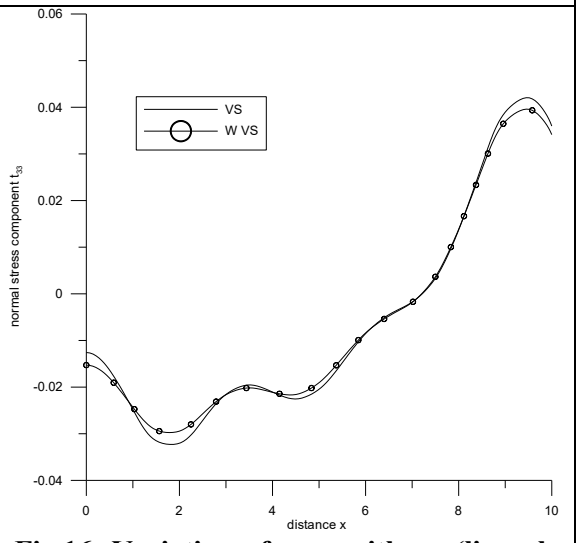

Fig.16. Variation of t_{33} with x (linearly distributed thermal source)

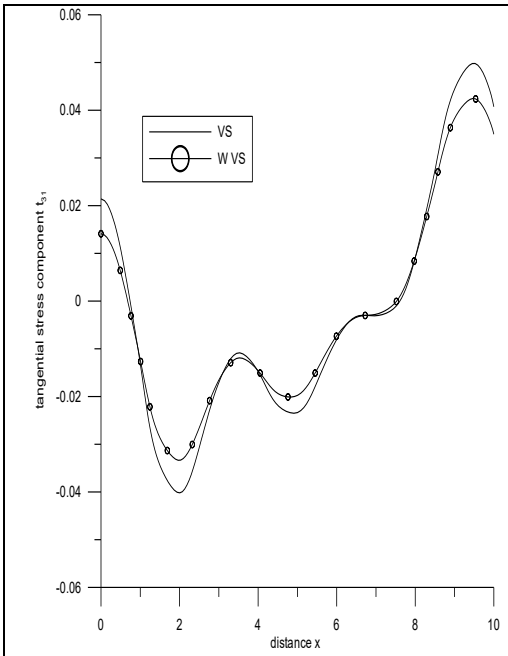

Fig.17 Variation of t_{31} with x (linearly distributed thermal source)

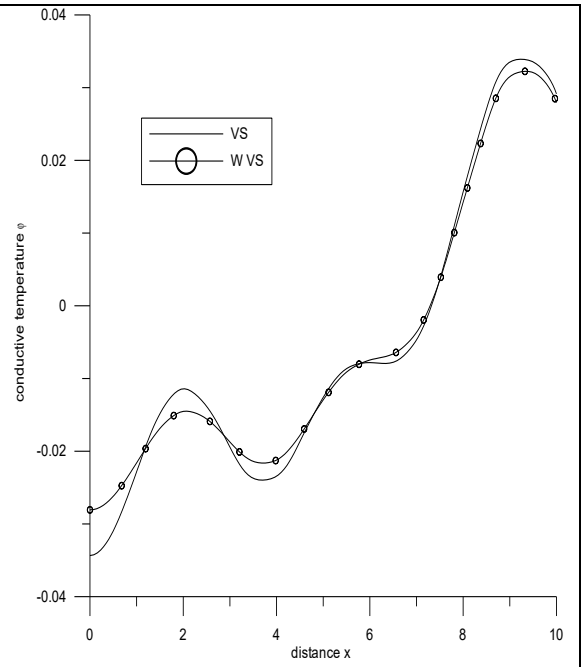

Fig.18 Variation of φ with x (linearly distributed thermal source)

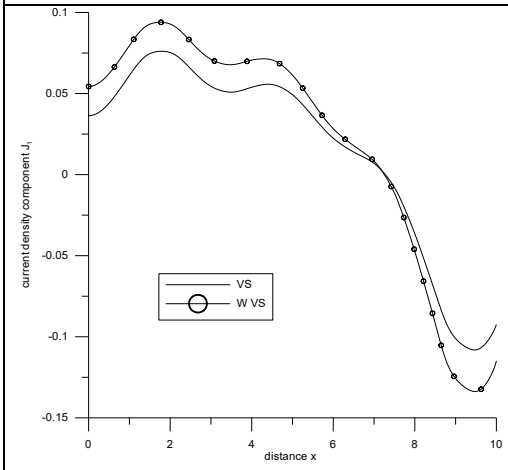

Fig.19 Variation of J_1 with x (linearly distributed thermal source)

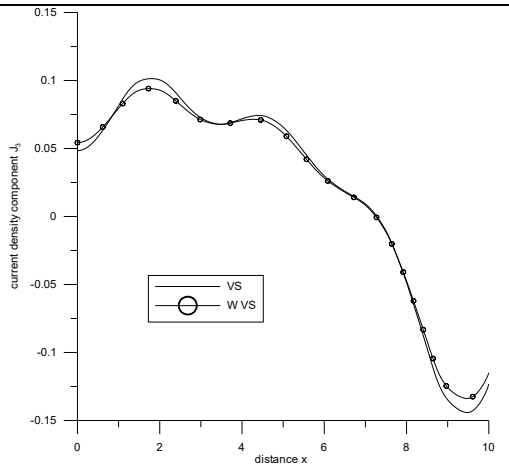

Fig.20 Variation of J_3 with x (linearly distributed thermal source)

Appendix A

$P = \delta_2\delta_3\zeta_7 + a_3\varepsilon_6\delta_2$

$Q = \zeta_{10}\zeta_7\delta_3 + \delta_2\zeta_7\zeta_{11} - \delta_3\delta_2\zeta_6 - \varepsilon_6{\beta_3}^2\zeta_4\delta_2 - \zeta_3^2\zeta_7 - i\xi a_3\zeta_3 p_3\varepsilon_6{\beta_1}^2 + \xi^2 a_3\varepsilon_6\delta_3{\beta_1}^2 - i\xi a_3\varepsilon_6\beta_1\beta_3\zeta_3 - \xi^2 a_3\varepsilon_6{\beta_1}^2\delta_3$

$R = \zeta_{10}\zeta_{11}\zeta_7 - \zeta_{10}\delta_3\zeta_6 - \varepsilon_6{\beta_3}^2\zeta_{10}\zeta_4 - \delta_2\zeta_6\zeta_{11} + \zeta_3^2\zeta_6 + \zeta_2^2\zeta_7 + p_3\zeta_3\zeta_4\varepsilon_6{\beta_1}^2 i\xi + i\xi\zeta_3\zeta_4\beta_1\beta_3\varepsilon_6 - \xi^2 a_3\zeta_{11}{\beta_1}^2\varepsilon_6$

$S = -\zeta_{10}\zeta_{11}\zeta_6 - \zeta_2^2\zeta_6 + \xi^2\zeta_{11}{\beta_1}^2\zeta_4\varepsilon_6$,

$\zeta_1 = -\left(\frac{M}{1+m^2}\mu_0 H_0 s + s^2\right) + \Omega^2$, $\zeta_2 = -\frac{M}{1+m^2}\mu_0 H_0 ms - 2\Omega s$, $\zeta_3 = (\delta_4 + \delta_2)i\xi$, $\zeta_4 = 1 + a_1\xi^2$,

$\zeta_6 = (\varepsilon_1 + \varepsilon_3\varepsilon_7 s)\xi^2 + s^2(1 + a_1\xi^2)$, $\zeta_7 = \varepsilon_2\varepsilon_7 + \varepsilon_4 s - a_1 s^2$, $\zeta_{10} = \zeta_1 - \xi^2$,

$\zeta_{11} = \zeta_1 - \delta_2\xi^2$,$\varepsilon_6 = \frac{T_0 s^2\,\varepsilon_7}{\rho^2 C_E c_1^2}$, $\varepsilon_7 = \left(1 + \tau_q\, s + \frac{\tau_q^2}{2!}s^2\right)$

Appendix B

$d_i = \frac{\lambda_i^2(\varepsilon_6 i\xi\delta_3 - \zeta_3\beta_3\beta_1\xi\,) - \lambda_i(\xi\beta_1\beta_3\zeta_2) + \varepsilon_6 i\xi\zeta_{11}}{\lambda_1^4(\delta_3\zeta_7 + a_3\varepsilon_6{\beta_3}^2) + \lambda_1^2(\zeta_7\zeta_{11} - \delta_3\zeta_6 - {\beta_3}^2\varepsilon_6\zeta_4) - \zeta_6\zeta_{11}}$ $i = 1,2,3$

$l_i = \frac{-\lambda_i^3(\zeta_3\zeta_7 + \varepsilon_6 i\xi\zeta_5 p_3) - \zeta_2\zeta_7\lambda_i^2 + (\zeta_3\zeta_6 + \varepsilon_6 i\xi p_3\zeta_4)\lambda_i + \zeta_6\zeta_2}{\lambda_1^4(\delta_3\zeta_7 + a_3\varepsilon_6{\beta_3}^2) + \lambda_1^2(\zeta_7\zeta_{11} - \delta_3\zeta_6 - {\beta_3}^2\varepsilon_6\zeta_4) - \zeta_6\zeta_{11}}$ $i = 1,2,3$

Appendix C

$\hat{u}_1 = \frac{-F_1\hat{\psi}_1(\xi,s)}{\Delta}\left(\Delta_1 e^{-\lambda_1 x_3} + \Delta_2 e^{-\lambda_2 x_3} + \Delta_3 e^{-\lambda_3 x_3}\right) + \frac{F_2\hat{\psi}_2(\xi,s)}{\Delta}\left(\Delta_1^* e^{-\lambda_1 x_3} + \Delta_2^* e^{-\lambda_2 x_3} + \Delta_3^* e^{-\lambda_3 x_3}\right)$(C.1)

$\hat{u}_3 = \frac{-F_1\hat{\psi}_1(\xi,s)}{\Delta}\left(d_1\Delta_1 e^{-\lambda_1 x_3} + d_2\Delta_2 e^{-\lambda_2 x_3} + d_3\Delta_3 e^{-\lambda_3 x_3}\right) + \frac{F_2\hat{\psi}_2(\xi,s)}{\Delta}\left(d_1\Delta_1^* e^{-\lambda_1 x_3} + d_2\Delta_2^* e^{-\lambda_2 x_3} + d_3\Delta_3^* e^{-\lambda_3 x_3}\right)$ (C.2)

$\hat{t}_{33} = \frac{-F_1\hat{\psi}_1(\xi,s)}{\Delta}\left(\Delta_{11}\Delta_1 e^{-\lambda_1 x_3} + \Delta_{12}\Delta_2 e^{-\lambda_2 x_3} + \Delta_{13}\Delta_3 e^{-\lambda_3 x_3}\right) + \frac{F_2\hat{\psi}_2(\xi,s)}{\Delta}\left(\Delta_{11}\Delta_1^* e^{-\lambda_1 x_3} + \Delta_{12}\Delta_2^* e^{-\lambda_2 x_3} + \Delta_{13}\Delta_3^* e^{-\lambda_3 x_3}\right)$ (C.3)

$c = \frac{-F_1\hat{\psi}_1(\xi,s)}{\Delta}\left(\Delta_{21}\Delta_1 e^{-\lambda_1 x_3} + \Delta_{22}\Delta_2 e^{-\lambda_2 x_3} + \Delta_{23}\Delta_3 e^{-\lambda_3 x_3}\right) + \frac{F_2\hat{\psi}_2(\xi,s)}{\Delta}\left(\Delta_{21}\Delta_1^* e^{-\lambda_1 x_3} + \Delta_{22}\Delta_2^* e^{-\lambda_2 x_3} + \Delta_{23}\Delta_3^* e^{-\lambda_3 x_3}\right)$ (C.4)

$\hat{\varphi} = \frac{-F_1\hat{\psi}_1(\xi,s)}{\Delta}\left(\Delta_{31}\Delta_1 e^{-\lambda_1 x_3} + \Delta_{32}\Delta_2 e^{-\lambda_2 x_3} + \Delta_{33}\Delta_3 e^{-\lambda_3 x_3}\right) + \frac{F_2\hat{\psi}_2(\xi,s)}{\Delta}\left(\Delta_{31}\Delta_1^* e^{-\lambda_1 x_3} + \Delta_{32}\Delta_2^* e^{-\lambda_2 x_3} + \Delta_{33}\Delta_3^* e^{-\lambda_3 x_3}\right)$ (C.5)

$\hat{J}_1 = \frac{-F_1\hat{\psi}_1(\xi,s)}{\Delta}\frac{c_1\sigma_0 H_0\mu_0}{1+m^2}\left((m - d_1)\Delta_1 e^{-\lambda_1 x_3} + (m - d_2)\Delta_2 e^{-\lambda_2 x_3} + (m - d_3)\Delta_3 e^{-\lambda_3 x_3}\right) + \frac{F_2\hat{\psi}_2(\xi,s)}{\Delta}\frac{c_1\sigma_0 H_0\mu_0}{1+m^2}\left((m - d_1)\Delta_1^* e^{-\lambda_1 x_3} + (m - d_2)\Delta_2^* e^{-\lambda_2 x_3} + (m - d_3)\Delta_3^* e^{-\lambda_3 x_3}\right)$ (C.6)

$\hat{J}_3 = \frac{-F_1\hat{\psi}_1(\xi,s)}{\Delta}\frac{c_1\sigma_0 H_0\mu_0}{1+m^2}\left((1 + md_1)\Delta_1 e^{-\lambda_1 x_3} + (1 + md_2)\Delta_2 e^{-\lambda_2 x_3} + (1 + md_3)\Delta_3 e^{-\lambda_3 x_3}\right) + \frac{F_2\hat{\psi}_2(\xi,s)}{\Delta}\frac{c_1\sigma_0 H_0\mu_0}{1+m^2}\left((1 + md_1)\Delta_1^* e^{-\lambda_1 x_3} + (1 + md_2)\Delta_2^* e^{-\lambda_2 x_3} + (1 + md_3)\Delta_3^* e^{-\lambda_3 x_3}\right)$ (C.7)

where $(\Delta_{22}\Delta_{33} - \Delta_{23}\Delta_{32}) = \Delta_1$, $(\Delta_{23}\Delta_{31} - \Delta_{21}\Delta_{33}) = \Delta_2$, $(\Delta_{21}\Delta_{32} - \Delta_{22}\Delta_{31}) = \Delta_3$

, $\sqrt{\xi^2 + \frac{c_1^2}{c^2}s^2} = \lambda_4$

$(\Delta_{12}\Delta_{23} - \Delta_{13}\Delta_{22}) = \Delta_1^*$, $(\Delta_{11}\Delta_{23} - \Delta_{13}\Delta_{21}) = \Delta_2^*$, $(\Delta_{11}\Delta_{22} - \Delta_{12}\Delta_{21}) = \Delta_3^*$

$\Delta_{1j} = \frac{c_{13}}{\rho c_1^2} i\xi - \frac{c_{33}}{\rho c_1^2} d_j\lambda_j - \frac{\beta_3}{\beta_1} l_j + \frac{\beta_3}{\beta_1} a_3 l_j \lambda_j{}^2 - \frac{\beta_3}{\beta_1} l_j a_1 \xi^2 \quad j = 1,2,3$

$\Delta_{2j} = -\lambda_j + i\xi d_j \quad j = 1,2,3$,

$\Delta_{3j} = -\lambda_j l_j, \qquad j = 1,2,3$

References:

[1] Lord, H. W., & Shulman, Y. (1967). A generalized dynamical theory of thermoelasticity. Journal of the Mechanics and Physics of Solids, 15(5), 299–309. https://doi.org/10.1016/0022-5096(67)90024-5

[2] Green, A. E., & Lindsay, K. A. (1972). Thermoelasticity. Journal of Elasticity, 2, 1–7. https://doi.org/10.1007/BF00045689

[3] Green, A. E., & Naghdi, P. M. (1991). A re-examination of the basic postulates of thermomechanics. Proceedings of the Royal Society of Londan. Series A:Mathematical and Physical Sciences, 432(1885), 171–194.

[4] Green, A. E., & Naghdi, P. M. (1992). On undamped heat waves in an elastic solid. Journal of Thermal Stresses, 15(2), 253–264.

[5] Green, A. E., & Naghdi, P. M. (1993). Thermoelasticity without energy dissipation. Journal of Elasticity, 31(3), 189–208.

[6] Chen, P. J., & Gurtin, M. E. (1968). On a theory of heat conduction involving two parameters. ZAMP, 19(4), 614–627.

[7] Chen, P. J., Gurtin, M. E., & Williams, W. O. (1968). A note on non-simple heat conduction. ZAMP, 19(6), 969–970.

[8] Chen, P. J., Gurtin, M. E., & Williams, W. O. (1969). On the thermodynamics of non-simple elastic materials with two temperatures. ZAMP, 20(1), 107–112.

[9] Warren, W. E., & Chen, P. J. (1973). Wave propagation in the two-temperature theory of thermoelasticity. Acta Mechanica, 16(1–2), 21–33.

[10] Youssef, H. M. (2006). Theory of two-temperature generalized thermoelasticity. IMA Journal of Applied Mathematics, 71(3), 383–390.

[11] Youssef, H. M., & Al-Lehaibi, E. A. (2007). State-space approach of two-temperature generalized thermoelasticity for a one-dimensional problem. International Journal of Solids and Structures, 44(5–6), 1550–1562.

[12] Youssef, H. M., & Al-Harby, A. H. (2007). State-space approach of two-temperature generalized thermoelasticity of an infinite body with a spherical cavity subjected to different types of thermal loading. Archive of Applied Mechanics, 77(9), 675–687.

[13] Youssef, H. M. (2011). Theory of two-temperature thermoelasticity without energy dissipation. Journal of Thermal Stresses, 34(2), 138–146.

[14] Youssef, H. M. (2013). Variational principle of two-temperature thermoelasticity without energy dissipation. Journal of Thermoelasticity, 1(1), 42–44.

[15] Ezzat, M. A., & Awad, E. S. (2010). Constitutive relations, uniqueness of solution, and thermal shock application in the linear theory of micropolar generalized thermoelasticity involving two temperatures. Journal of Thermal Stresses, 33(3), 226–250.

[16] Kaushal, S., Sharma, N., & Kumar, R. (2010). Propagation of waves in generalized thermoelastic continua with two temperatures. International Journal of Applied Mechanics and Engineering, 15(4), 1111–1127.
[17] Sharma, K. (2010). Boundary value problems in generalized thermodiffusive elastic medium. Journal of Solid Mechanics, 2(5), 348–362.
[18] Sharma, K. (2011). Analysis of deformation due to inclined load in generalized thermodiffusive elastic medium. International Journal of Engineering, Science and Technology, 3(2), 117-129.
[19] Kaushal, S., Kumar, R., & Miglani, A. (2011). Wave propagation in temperature rate dependent thermoelasticity with two temperatures. Mathematical Sciences, 5(2), 125–146.
[20] Sharma, N., Kumar, R., & Ram, P. (2012). Interactions of generalized thermoelastic diffusion due to inclined load. International Journal of Emerging Trends in Engineering and Development, 5(2), 583–600.
[21] Sharma, K., & Marin, M. (2013). Effect of distinct conductive and thermodynamic temperatures on the reflection of plane waves in micropolar elastic half space. UPB Scientific Bulletin, 75(2), 121–132.
[22] Abbas, I. A., Kumar, R., & Reen, L. S. (2014). Response of thermal sources in transversely isotropic thermoelastic materials without energy dissipation and with two temperatures. Canadian Journal of Physics, 92(11), 1305–1311.
[23] Sharma, S., & Sharma, K. (2014). Influence of heat sources and relaxation time on temperature distribution in tissues. International Journal of Applied Mechanics and Engineering, 19(2). 427-433.
[24] Atwa, S. Y., & Jahangir, A. (2014). Two-temperature effects on plane waves in generalized thermomicrostretch elastic solids. International Journal of Thermophysics, 35(1), 175–193.
[25] Kumar, R., & Rupender. (2009). Effect of rotation in magneto-micropolar thermoelastic medium due to mechanical and thermal sources. Chaos, Solitons & Fractals, 41(3), 1619–1633.
[26] Kumar, R., & Devi, S. (2010). Magnetothermoelastic (Type II AND III) half-space in contact with vacuum. Applied Mathematical Sciences, 4(69), 3413–3424.
[27] Mahmoud, S. R. (2013). An analytical solution for effect of magnetic field and initial stress on an infinite generalized thermoelastic rotating nonhomogeneous diffusion medium. Abstract and Applied Analysis, 2013. 1-13.
[28] Das, P., & Kanoria, M. (2014). Study of finite thermal waves in a magnetothermoelastic rotating medium. Journal of Thermal Stresses, 37(4), 405–428.
[29] Freudenthal, A. M. (1954). Effect of rheological behavior on thermal stresses. Journal of Applied Physics, 25(9), 1110–1117.
[30] Ieşan, D., & Scalia, A. (1989).Some theorems in the theory thermoviscoelasticity. Journal of Thermal Stresses, 12(2), 225–239.
[31] Borrelli, A., & Patria, M. C. (1991). Discontinuity waves in thermoviscoelastic solids. International Journal of Non-Linear Mechanics, 26(2), 141–150.
[32] Ezzat, M. A., & Atef, H. M. (2011). Magneto-thermo-viscoelastic material with cavity. Journal of Civil Engineering, 2(1), 6–16.
[33] Abd-Allaa, A. M., & Mahmoud, S. R. (2011). Magneto-thermo-viscoelastic interactions. Applied Mathematical Sciences, 5(29), 1431–1447.

[34] Kumar, R., Chawla, V., & Abbas, I. A. (2012). Effect of viscosity on wave propagation in anisotropic thermoelastic medium with three phase-lag- model. Theoretical and Applied Mechanics, 39(4), 313–341.
[35] Sharma, S., Sharma, K., & Bhargava, R. R. (2013). Effect of viscosity on wave propagation in anisotropic thermoelastic with Green-Naghdi theory type-II and type-III. Materials Physics and Mechanics, 16(2), 144–158.
[36] Sharma, S., Sharma, K., & Bhargava, R. R. (2013). Wave motion in electro-microstretch solids. Materials Physics and Mechanics, 17(1), 93–110.
[37] Sharma, K., & Kumar, P. (2013). Plane waves in thermoviscoelastic medium. Journal of Thermal Stresses, 36(1), 94–111.
[38] Sharma, K., & Bhargava, R. R. (2014). Thermoelastic plane waves at imperfect boundary. Afrika Mathematika, 25(1–2), 81–102.
[39] Hilton, H. H. (2014). Coupled longitudinal one-dimensional thermal and viscoelastic waves in media with temperature-dependent material properties. Engineering Mechanics, 21(4), 219–238.
[40] Al-Basyouni, K. S., Mahmoud, S. R., & Alzahrani, E. O. (2014). Effect of rotation, magnetic field, and periodic loading on radial vibrations of thermo-viscoelastic non-homogeneous media. Boundary Value Problems, 2014. 1-11.
[41] Yadav, R., Kalkal, K., & Deswal, S. (2015). Two-temperature generalized thermoviscoelasticity with fractional-order strain subjected to a moving heat source: State-space approach. Journal of Mathematics, 2015,1-13.
[42] Zakaria, M. (2012). Effects of Hall current and rotation on magneto-micropolar generalized thermoelasticity due to ramp-type heating. International Journal of Electromagnetics, 2(3), 24–32.
[43] Sarkar, N., & Lahiri, A. (2012). Temperature rate-dependent generalized thermoelasticity with modified Ohm's law. International Journal of Computational Materials Science, 1(4), 1250031.
[44] Zakaria, M. (2014). Effect of Hall current on generalized magneto-thermoelasticity micropolar solid subjected to ramp-type heating. International Applied Mechanics, 50(1), 92-104.
[45] Kumar, R., Devi, S., & Sharma, V. (2017). Effect of Hall current and rotation in modified couple stress generalized thermoelastic half-space due to ramp-type heating. Journal of Solid Mechanics, 9(3), 527–542.
[46] Chandrasekharaiah, D. S. (1998). Hyperbolic thermoelasticity: A review of recent literature. Applied Mechanics Reviews, 51, 705–729.
[47] Kumar, R., Sharma, N., & Lata, P. (2017). Effects of Hall current and two temperatures in transversely isotropic magnetothermoelastic with and without energy dissipation due to ramp type heat. Mechanics of Advanced Materials and Structures, 24(8), 625–635.
[48] Lata, P. (2017). A comparison between isotropic and transversely isotropic thermoelastic solids with two temperature and without energy dissipation in frequency domain due to concentrated force. International Journal of Mechanics and Solids, 9(1), 77–88.
[49] Ezzat, M. A., & El-Bary, A. A. (2017). Fractional magneto-thermoelastic materials with phase lag Green–Naghdi theories. Steel and Composite Structures, 24(3), 297–307.

[50] Ezzat, M. A., El-Karamany, A. S., & El-Bary, A. A. (2018). Two-temperature theory in Green–Naghdi thermoelasticity with fractional phase-lag heat transfer. Microsystem Technologies, 24(2), 951–961.
[51] Lata, P., & Kaur, I. (2018). Effect of Hall current in transversely isotropic magnetothermoelastic rotating medium with fractional order heat transfer due to normal force. Advances in Materials Research, 7(3), 203–220.
[52] Slaughter, W. S. (2002). The linearised theory of elasticity. Birkhäuser.
[53] Kaliski, S. (1963). Absorption of magneto-viscoelastic surface waves in a real conductor magnetic field. Proceedings of Vibration Problems, 4, 319-329.
[54] Honig, G., & Hirdes, U. (1984). A method for the numerical inversion of Laplace transform. Journal of Computational and Applied Mathematics, 10, 113–132.
[55] Press, W. H., Teukolsky SA, Vetterling WT, & Flannery BP (1986). Numerical recipes in Fortran. Cambridge University Press, Cambridge.
[56] Dhaliwal, R. S., & Singh, A. (1980). Dynamic coupled thermoelasticity. Hindustan Publisher Corporation, New Delhi.